Magnet-less Non-Reciprocal Bandpass Filters With Tunable Center Frequency

Dakotah Simpson and Dimitra Psychogiou

Dept. of Electrical, Computer, and Energy Engineering, University of Colorado Boulder, USA

{Dakotah.Simpson, Dimitra.Psychogiou}@colorado.edu

***Abstract* — This paper reports on the RF design of non-reciprocal magnet-less bandpass filters (BPFs) with continuously tunable center frequency. It is shown that by modulating the resonant frequencies of the BPF resonators with progressively shifted AC signals, the RF signal propagation in the overall BPF is enabled in one direction—e.g., from port 1-to-2—whereas it is sufficiently suppressed in the reverse one. The operating principles of the magnet-less non-reciprocal BPF concept are demonstrated through circuit-based analysis of a three-resonator BPF. For practical validation purposes, a lumped-element proof-of-concept prototype was designed, manufactured, and tested at 140 MHz. It demonstrated minimum in-band insertion loss in the forward direction of 3.7 dB, maximum isolation of up to 52.8 dB in the reverse direction, and center frequency tuning from 136 MHz to 163 MHz (1.2:1 tuning).**

***Keywords* — Bandpass filter (BPF), lumped-element filter, non-reciprocal filter, non-reciprocity, tunable filter.**

I. Introduction

Non-reciprocal RF devices such as isolators and circulators are among the most important components of the RF front-ends of wireless communication and radar systems due to their ability to i) protect sensitive RF devices against reflected signals and to ii) facilitate simultaneous transmit and receive operation in full-duplex radios. Their operation is based on non-reciprocal RF signal transmission between their input/output ports that is typically achieved by incorporating ferromagnetic materials within their volume. Despite the high levels of isolation that can be obtained with these devices, they exhibit large physical size due to the need for external magnet biasing that inhibits their integration with IC-based components.

In an effort to overcome the aforementioned limitations, recent research efforts are focusing in the development of magnet-free non-reciprocal devices either by incorporating unilateral transistor-based elements within the volume of RF circulators/isolators or by breaking the time-reversal symmetry [1]-[6]. Spatiotemporal modulation is a technique in which the time-reversal symmetry is broken by modulating a circuit in both space (e.g., a medium and/or resonators) and in time with a time-varying signal. The circulator-design approaches in [1], [2], demonstrate the potential to achieve non-reciprocity by introducing angular momentum biasing into the resonators of inter-connected resonant rings. In particular, the resonant frequencies of the resonators are modulated by signals that have a progressive phase shift of 120° (relative to the previous resonator). The use of transistor-based stages within the circulator/isolator volume has also been demonstrated for the realization of non-reciprocity [3], [4]. However, these devices typically suffer from poor noise performance and strong nonlinearities. In yet another configuration, linear periodically time-variant *N*-path filters break reciprocity through staggered commutation [5].

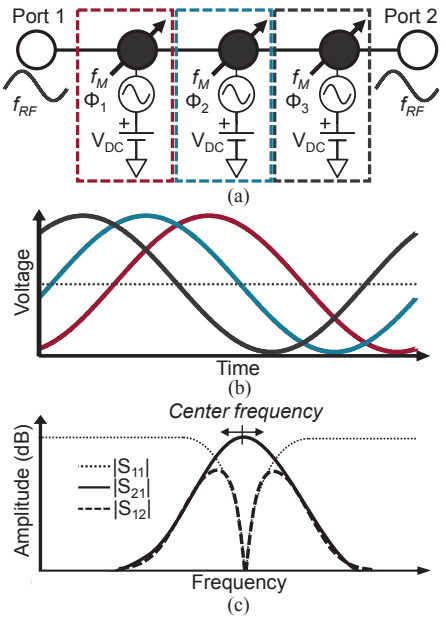

Fig. 1. Tunable magnet-less non-reciprocal BPF concept based on modulated RF resonators. Non-reciprocity is achieved by altering in time the resonant frequency of its constituent resonators through appropriately phased AC signals with $f_M << f_{RF}$. Center frequency tuning is realized by altering the DC resonator biasing. (a) Coupling-routing diagram. White circles: input and output; black circles: frequency-tunable, f_M-modulated, DC-biased resonators with external AC sources. (b) Conceptual illustration of the AC modulation signals applied on the DC-biased resonator varactors. (c) Conceptual power transmission (S_{21}), reflection (S_{11}), and isolation (S_{12}) responses of the magnet-less non-reciprocal BPF.

Despite significant research efforts in the development of magnet-less circulators and isolators with the purpose of miniaturizing the size of the RF front-end, its size is additionally dictated by the off-chip bandpass filters (BPFs) that are placed between the antenna interface and the active stages (e.g., PA, LNA). In an effort to further reduce the RF front-end size, this paper reports for the first time on the development of a new type of tunable BPFs with non-reciprocal

behaviour—i.e., co-designed RF filtering and isolation functionality—that eliminates the need for an isolator. Non-reciprocity is achieved by modulating the resonant frequencies of the BPF's resonators with progressively phased AC signals. Center frequency tunability is also shown, allowing for additional levels of miniaturization in the RF front-end.

The rest of this manuscript is organized as follows. In Section II, the main operational and design principles of the proposed non-reciprocal BPF concept are presented through circuit-based simulations. The RF design and experimental testing of a lumped-element three-resonator BPF prototype with a center frequency of 140 MHz and 1.2:1 tuning range are reported in Section III. Lastly, a summary of the main contributions of this work is given in Section IV.

II. Operating Principles

The coupling-routing diagram and conceptual power transmission, isolation, and reflection responses of the proposed tunable non-reciprocal BPF are shown in Fig. 1. As it can be seen in Fig. 1(a), the filter is comprised of three frequency-tunable resonators whose resonant frequencies are altered by applying DC and AC biasing on their constituent varactor-based capacitors. Whereas the DC biasing sets the nominal resonator capacitance and defines the BPF's center frequency, the time-dependent AC biasing controls the directionality of the RF signal propagation within the BPF volume. By appropriately selecting the frequency f_M of the AC signal that modulates the capacitance of the BPF resonators and by assigning a progressive phase difference between the AC signals—Fig. 1(b)—of the BPF's resonators, non-reciprocity can be achieved in the overall BPF transfer function, Fig. 1(c). Considering a reference phase of zero for the AC signal applied at the first resonator Φ_1, Φ_2 denotes the phase difference between the second and the first resonator and Φ_3 the phase difference between the third and the first so that $\Phi_3 > \Phi_2 > \Phi_1 = 0$.

Fig. 2 shows the circuit-equivalent representation of the proposed three-resonator BPF along with the AC/DC biasing scheme that allows for spatiotemporal modulation. In particular, each resonator is made of a pair of varactor diodes, D_V, that are connected in parallel to a static capacitor, C_R. The varactors act as the tuning element in the resonator and are responsible for varying its resonant frequency. In order for simultaneous DC and AC biasing to be applied on the resonators' varactors, their corresponding biasing network needs to be designed as follows. A series LC resonator (C_M and L_M) that resonates at f_M is used for the connection of the AC source in order to prevent any RF signal to leak to the AC source. The DC biasing is applied through an RF choke inductor (L_{DC}) and a capacitor to ground (C_{DC}) to further reject any RF signal from entering to the DC supply.

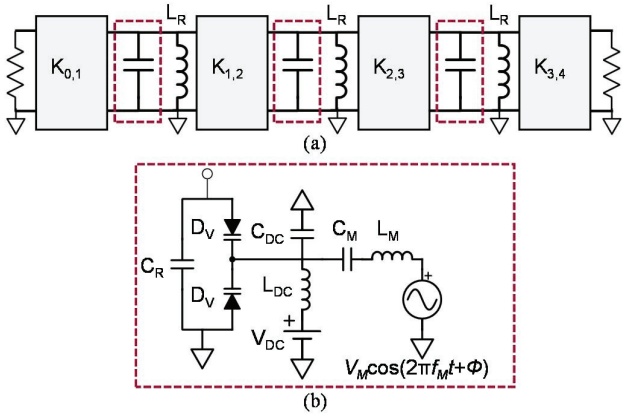

Fig. 2. Circuit-schematic of the non-reciprocal three-resonator BPF. (a) Overall architecture consisting of three parallel LC resonators coupled through impedance inverters. (b) Detailed schematic of the capacitor network that allows for resonant frequency modulation.

The non-reciprocal filter design is performed as follows. At first, the BPF is designed for the desired center frequency and bandwidth (BW) using conventional coupled-resonator RF design techniques and without considering any type of AC modulation. Having defined the required resonator capacitance, the appropriate DC biasing point is selected for the resonator varactors. Afterwards the AC modulation parameters—f_M, V_M, and progressive phase shift offsets Φ_2 and Φ_3 are obtained through optimization with the purpose of achieving optimum RF performance in terms of minimum in-band insertion loss (IL) in the forward transmission and maximum isolation in the reverse transmission.

In order to illustrate the aforementioned design steps, a three-resonator BPF design is considered for center frequency of 140 MHz and a BW of 35 MHz (25%). Its circuit-based simulated response without the presence of AC modulation is shown in Fig. 3 using commercially available varactors, Skyworks SMV1265, and ideal RF components. The simulations were completed using the software package Advanced Design System (ADS) from Keysight Technologies. The BPF response in the presence of AC modulation is illustrated in Fig. 4 for various important RF design parameters—f_M, V_M, $\Phi_{1\text{-}3}$—. In particular, Fig. 4(a) shows how the BPF response changes with varying f_M. As it can be seen, too low of a modulation frequency results in high IL and low isolation levels in the reverse transmission. On the contrary, higher modulation frequencies result in only low isolation. Maximum isolation and minimum IL is obtained for a modulation frequency of 20 MHz. From this observation, it can be concluded that $f_M \approx BW/2$. Fig. 4(b) illustrates variations in the phase offset of the AC sources which affect both the

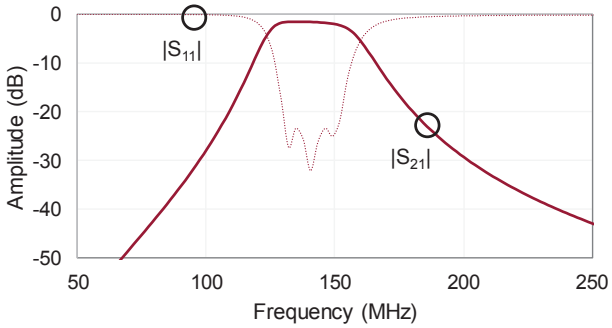

Fig. 3. Simulated BPF frequency response without modulating the capacitance of the BPF resonators that results in a reciprocal behaviour, i.e., $|S_{21}|=|S_{12}|$. In this example, $K_{0,1}=K_{3,4}=0.36$, $K_{1,2}=K_{2,3}=0.11$, $L_R=93$ nH, $C_R=5.6$ pF, and $V_{DC}=0.9$ V.

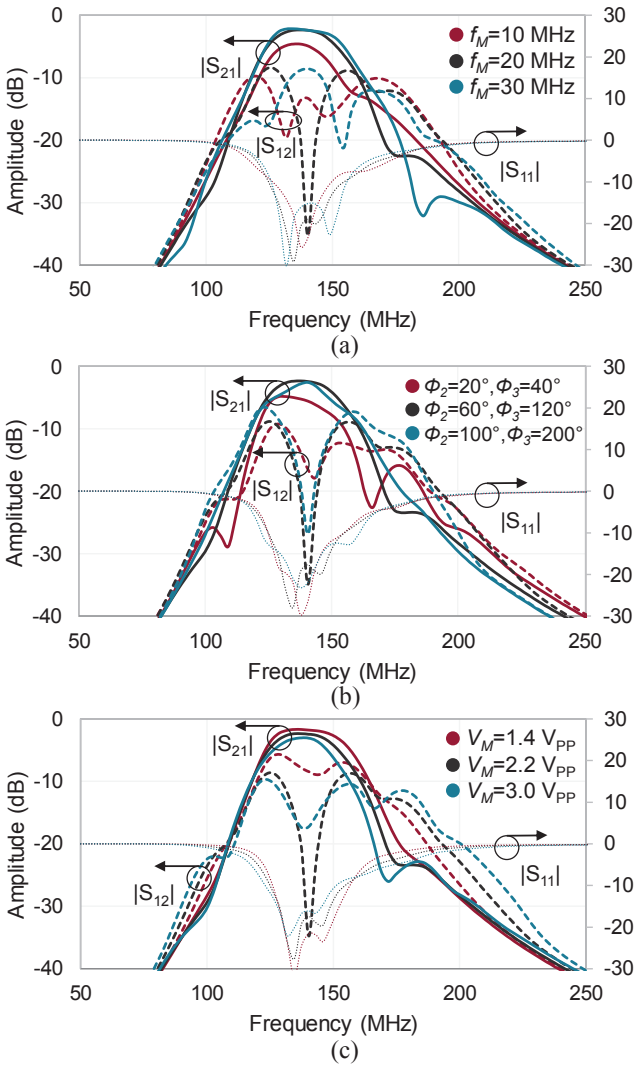

Fig. 4. Simulated power transmission and reflection responses of the third-order BPF with spatiotemporal modulation for alternative levels of the modulation parameters. (a) Variations of modulation frequency, f_M. Φ_2=60°, Φ_3=120°, V_M=2.2 V_{PP}. (b) Variations of phase offsets, Φ_2 and Φ_3. f_M=20 MHz, V_M=2.2 V_{PP}. (c) Variations of the magnitude of the modulation signals, V_M. f_M=20 MHz, Φ_2=60°, Φ_3=120°. In all responses: $K_{0,1}$=$K_{3,4}$=0.36, $K_{1,2}$=$K_{2,3}$=0.11, L_R=93 nH, C_R=5.6 pF, L_M=100 µH, C_M=0.57 pF, and V_{DC}=0.9 V.

isolation and IL as well as the passband symmetry. As it can be seen, the highest isolation and most symmetric BPF response is achieved when Φ_2=60° and Φ_3=120°. Lastly, Fig. 4(c) demonstrates variations in the modulation signal magnitude V_M for AC signals with Φ_2=60° and Φ_3=120°. As it can be seen, low V_M values result in BPFs with wider BWs and lower isolation. For the particular BPF design, a magnitude of about 2.2 V_{PP} demonstrates the best performance in terms of IL and isolation.

III. Experimental Results

To experimentally validate the proposed non-reciprocal BPF concept, a lumped-element three-resonator prototype was

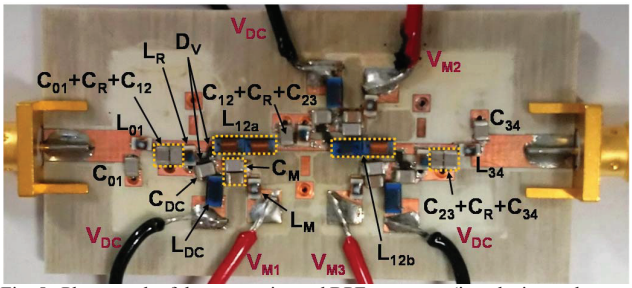

Fig. 5. Photograph of the non-reciprocal BPF prototype (i.e., device under test, DUT). C_{01}=C_{34}=9.1 pF, L_{01}=L_{34}=150 nH, C_{01}+C_R+C_{12}=17.1 pF, L_R=82 nH, C_{DC}=68 pF, L_{DC}=120 nH, C_M=200 pF, L_M=150 nH, L_{12a}=360 nH, C_{12}+C_R+C_{23}=12 pF, L_{12b}=280 nH, C_{23}+C_R+C_{34}=17.5 pF.

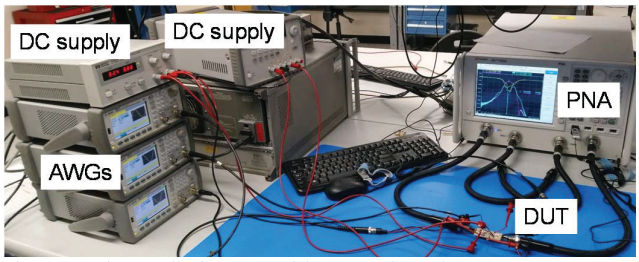

Fig. 6. RF-characterization setup of the non-reciprocal BPF prototype.

designed, manufactured, and measured. It was designed at a center frequency of 140 MHz and was built on a Rogers RO4003C substrate (thickness H=1.52mm, relative permittivity ε_r=3.38, and dielectric loss tangent tanδ_D=0.0027). The design was performed in ADS while using the RF design trade-offs in Section II. The impedance inverters were realized with their lowpass pi-type circuit equivalent. SMV1265 varactors from Skyworks were utilized as tuning and modulation elements of the BPF's resonators. Photographs of the non-reciprocal BPF prototype and of the RF characterization setup are shown in Figs. 5 and 6, respectively. For the modulated signals, three clock-synced arbitrary-waveform generators (AWGs) are used. The transmission, isolation, and reflection responses are measured in terms of S-parameters using a Keysight N5224A PNA.

The RF-measured response of the non-reciprocal BPF along with a comparison of its EM-simulated one is shown in Fig. 7. As it can be seen, they are in a good agreement, successfully validating the proposed non-reciprocal BPF concept. The

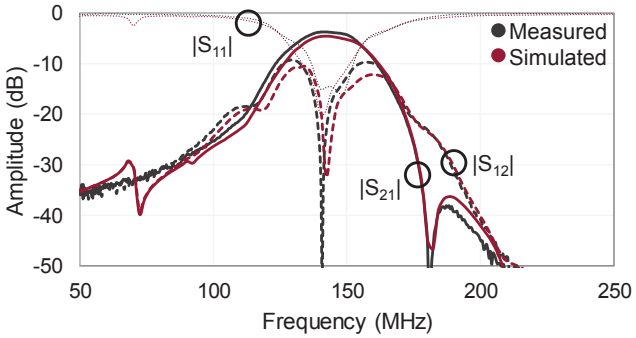

Fig. 7. Comparison of the RF-measured and EM-simulated power transmission and reflection responses of the manufactured prototype in Fig. 5.

measured center frequency and BW are 143 MHz and 27.5 MHz (19.2%), respectively. The minimum in-band IL of the forward transmission response ($|S_{21}|$) was measured to be 3.7 dB while the maximum isolation in the reverse direction ($|S_{12}|$) was measured to be 52.8 dB. Fig. 8 compares the responses of the prototype in a wide frequency range when the modulation is turned on and off. As can be seen, the IL and center frequency remain relatively constant in both states. However, the BW is slightly reduced when the modulation is turned on and a rounding effect is also observed. As expected, when the modulation is turned off, the filter exhibits a conventional reciprocal behaviour (i.e., $|S_{21}|=|S_{12}|$).

In order to examine the potential of tuning the center frequency of the non-reciprocal BPF, the DC bias voltage is uniformly altered on all three resonators. The obtained RF measured filter performance is shown in Fig. 9. As it can be seen, the center frequency can be tuned from 136 MHz to 163 MHz (i.e., 1.2:1 ratio) while retaining a non-reciprocal behaviour. For all depicted measured states, the isolation in the reverse direction was measured >20 dB and the IL and return loss in the forward direction were measured < 4.1 dB and >14 dB, respectively. Despite the IL in the passband being somewhat higher than that reported for static lumped-element BPFs, this is the first reported BPF with tunable center frequency and non-reciprocal behaviour. It demonstrates the potential to realize RF co-designed devices that simultaneously exhibit the RF processing action of a BPF and an RF isolator and pave the way to the realization of miniaturized RF front-end.

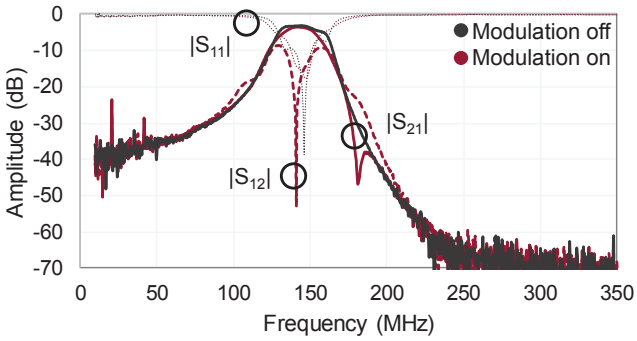

Fig. 8. Measured power transmission and reflection responses of the manufactured prototype in Fig. 5 when the modulation of the resonators' capacitances is turned on and off.

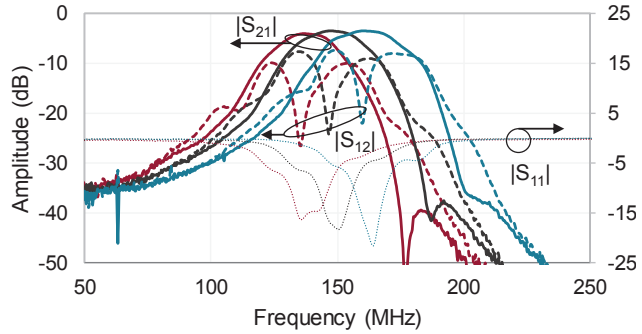

Fig. 9. RF-measured center frequency tuning of the manufactured prototype in Fig. 5 by adjusting the DC biasing voltage of the varactors.

IV. Conclusion

A new class of non-reciprocal magnet-less BPFs has been presented. They are based on modulated RF resonators whose resonant frequencies are altered through progressively phase-shifted AC signals that are applied on their constituent capacitors. In this manner, directionality is added within the BPF volume with increased levels of isolation between its forward and reverse transmission. The operational principles of the non-reciprocal BPF concept have been demonstrated through various parametric circuit-based simulations. For practical demonstration purposes, an experimental lumped-element three-resonator BPF prototype was designed, manufactured, and measured at 140 MHz. It exhibits a passband with minimum IL levels of 3.7 dB and up to 52.8 dB of isolation between its forward and reverse transmission paths. As an added advantage to be highlighted, the BPF's passband can be tuned within a 1.2:1 tuning range without losing its non-reciprocal behaviour.

Acknowledgment

This work has been supported in part by the National Science Foundation under award number 1731956 and the MTT-S Graduate Fellowship. The authors would like to thank Keysight for providing access to the software package ADS, Rogers Corporation for providing the Rogers RO4003C substrate, and Coilcraft Inc. for all the inductors .

References

[1] N. A. Estep, D. L. Sounas, and A. Alù, "Magnetless microwave circulators based on spatiotemporally modulated rings of coupled resonators," *IEEE Trans. Microw. Theory Techn.*, vol. 64, no. 2, pp. 502-518, Feb. 2016.

[2] A. Kord, D. L. Sounas, and A. Alù, "Differential magnetless circulator using modulated bandstop filters," *2017 IEEE MTT-S Intern. Microw. Symp. (IMS)*, Honolulu, HI, 2017, pp. 384-387.

[3] S. W. Y. Mung and W. S. Chan, "Active three-way circulator using transistor feedback network," *IEEE Microw. Wireless Compon. Lett.*, vol. 27, no. 5, pp. 476-478, May 2017.

[4] P. Chen and R. M. Narayanan, "Design of Active Circulators Using High-Speed Operational Amplifiers," *IEEE Microw. Wireless Compon. Lett.*, vol. 20, no. 10, pp. 575-577, Oct. 2010.

[5] N. Reiskarimian and H. Krishnaswamy, "Fully-integrated non-magnetic non-reciprocal components based on linear periodically-time-varying circuits," *2017 IEEE 17th Topical Meeting Silicon Monolithic Integrated Circuits in RF Systems (SiRF)*, Phoenix, AZ, 2017, pp. 111-114.

[6] M. Nafe, M. N. Hasan, H. Reggad, D. Kuzmenko, J. Chen, and X. Liu, "Magnetic-free circulator based on spatio-temporal modulation implemented via switched capacitors for full duplex communication," *2018 USNC-URSI Radio Science Meeting*, Boston, MA, 2018, pp. 119-120.